Nanoparticle networks reduce the flammability of polymer nanocomposites

TAKASHI KASHIWAGI[1]*, FANGMING DU[2], JACK F. DOUGLAS[3]*, KAREN I. WINEY[2], RICHARD H. HARRIS Jr[1] AND JOHN R. SHIELDS[1]

[1]Fire Research Division, National Institute of Standards and Technology, Gaithersburg, Maryland 20899-8665, USA
[2]Chemical and Biomolecular Engineering, University of Pennsylvania, Philadelphia, Pennsylvania 19104-6272, USA
[3]Polymers Division, National Institute of Standards and Technology, Gaithersburg, Maryland 20899-8544, USA
*e-mail: takashi.kashiwagi@nist.gov; jack.douglas@nist.gov

Published online: 23 October 2005; doi:10.1038/nmat1502

Synthetic polymeric materials are rapidly replacing more traditional inorganic materials, such as metals, and natural polymeric materials, such as wood. As these synthetic materials are flammable, they require modifications to decrease their flammability through the addition of flame-retardant compounds. Environmental regulation has restricted the use of some halogenated flame-retardant additives, initiating a search for alternative flame-retardant additives. Nanoparticle fillers are highly attractive for this purpose, because they can simultaneously improve both the physical and flammability properties of the polymer nanocomposite. We show that carbon nanotubes can surpass nanoclays as effective flame-retardant additives if they form a jammed network structure in the polymer matrix, such that the material as a whole behaves rheologically like a gel. We find this kind of network formation for a variety of highly extended carbon-based nanoparticles: single- and multiwalled nanotubes, as well as carbon nanofibres.

The burning process of a polymeric material typically begins with heating to a temperature at which thermal degradation initiates. The boiling temperatures of most of the thermal degradation products of polymers are much lower than the thermal degradation temperatures of thermoplastics, and the degradation products are then superheated as they form[1]. Bubbles nucleate below the heated polymer surface and grow with the supply of more degradation products by diffusion from the surrounding molten plastic[2], and they further evolve into the gas phase as fuel vapour. These bubbles agitate the outer layer of polymer melt and can interfere with the formation of a solid, char-like heat-transfer barrier at the boundary[1]. It has been recognized that the use of nanoscale reinforcing fillers, such as nanoclay particles, can help to reduce the flammability of polymeric materials by inhibiting this vigorous bubbling process in the course of degradation during combustion[1]. The addition of these filler particles often leads to the added benefit of enhancing the physical properties of nanocomposites relative to the polymer matrix[3–5]. On the other hand, this flame-retardant effect is not general for all nanocomposite additives. We previously found that poly(methyl methacrylate) (PMMA)/nanocomposites of nanosilica (13% mass fraction) showed vigorous bubbling during burning as in unfilled materials, leading ultimately to a residue consisting of granular, coarse particles[6]. The effect of these symmetric nanoparticles on flammability was only marginal for this class of fillers. In contrast, nanocomposites based on nanoclay particles formed a continuous protective solid layer on the burning surface or extended island structures made of clay and carbonaceous char during burning[7–10]. (Several review papers are available that describe the flame-retardant effect of these additives[11–14].) The presence of the protective layer is clearly important in the flammability reduction by these additives, but these clay-particle layers tend to develop large lateral surface cracks in which vigorous bubbling still occurs[15]. These extended nanoparticles are clearly promising flame retardants, but further studies are needed to improve the effectiveness of this type of filler and to understand the physical factors responsible for this flame-retardant effect.

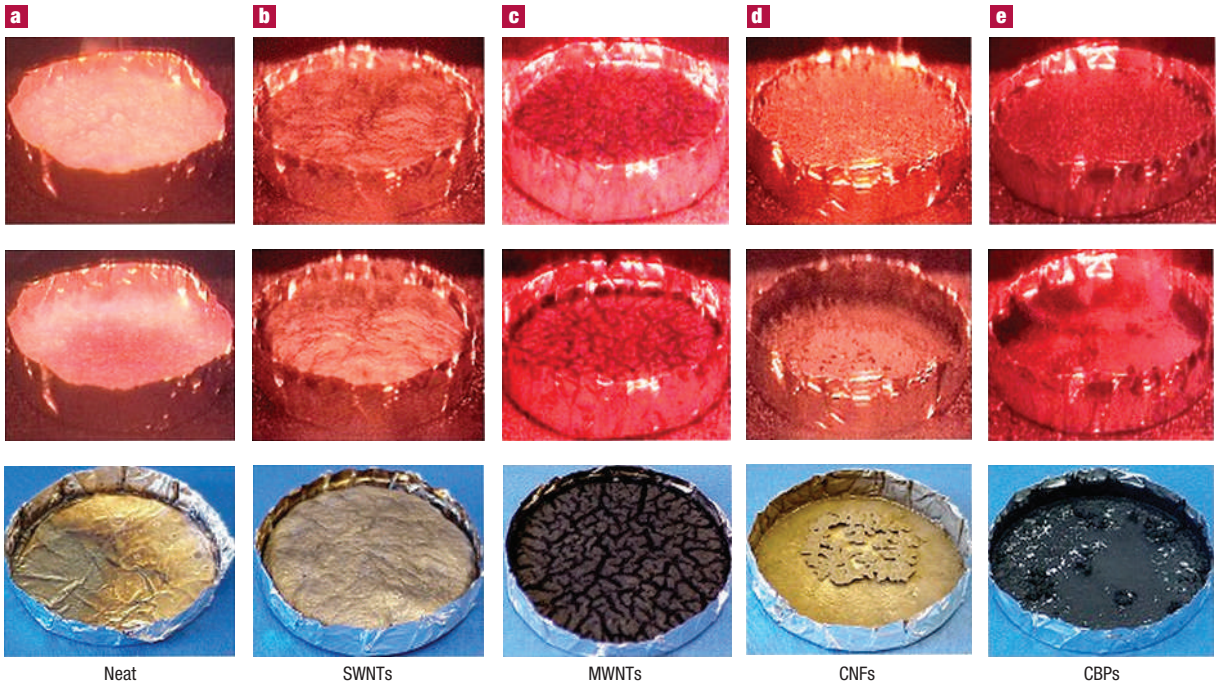

Figure 1 Selected sequences of sample behaviour during gasification and the collected residues. The top two rows are sample behaviour and the bottom row consists of pictures of the residues. The nanocomposite samples were PMMA with 0.5% mass fraction of each nanoparticle. The tests were conducted at 50 kW m^{-2} in nitrogen.

Polymer nanocomposites with low levels of single-walled carbon nanotubes (SWNTs)[16–19], multiwalled carbon nanotubes (MWNTs)[20–24] or carbon nanofibres (CNFs)[25–28] show significantly increased mechanical properties and electrical conductivity and, similarly to clay, they have a highly extended structure. Thus, carbon-based nanoadditives provide another attractive class of nanoparticle to be examined for flame retardancy. The combination of nanotubes with clay particles provides another class of materials worth exploration as flame-retardant additives[29,30].

We previously found that nanocomposites based on carbon nanotubes are likewise capable of forming a continuous network-structured protective layer without the formation of cracks that compromise the flame-retardant effectiveness. This resulted in a significant reduction in heat release rate (a flammability measure related to the fire intensity) with a carbon nanotube mass concentration as low as 0.5% (refs 31–33). This protective layer consisted mainly of carbon nanotubes and it seemed to act as a heat shield for the virgin polymer below the layer[32–34]. Poorly dispersed carbon nanotubes resulted in the formation of a discontinuous layer consisting of fragmented islands (with sizes from 1 to 10 mm) rather than the continuous network protective layer[33]. Very low concentrations of the tubes yielded the same fragmented island structures as found in the clay nanocomposite measurements. The flame-retardant performance of the nanocomposites containing the island structures was much poorer than that of the nanocomposites forming a continuous protective network layer. Thus, the formation of the network-structured protective layer during burning, without any openings or cracks, seems to be crucial for the large reduction in heat release rate. In the present study, we suggest that this network forms in the original sample under appropriate fabrication conditions and that this structure provides the main source of the protective layer that forms during the burning process. This hypothesis is systematically tested with various sizes and concentrations of carbon-based nanoparticles in a PMMA matrix.

The selected nanoparticles all had a common carbon chemistry: SWNTs, MWNTs and CNFs. The effects of the size of the tubes on the physical structure of the protective layer and on the flame-retardant effectiveness were determined. Carbon black particles (CBPs) were also included for comparison to gain insight into the role of particle anisotropy in the flame-retardant effect.

A selected sequence of video images of a sample during gasification tests is shown in Fig. 1 for an external radiant flux of 50 kW m^{-2} in nitrogen (no flaming but sample heating similar to fire conditions). The PMMA had a viscosity-average nominal molecular mass of 100,000 g mol^{-1} and the mass fraction of SWNTs, MWNTs, CNFs and CBPs was 0.5% in each case. Pristine PMMA behaved like a liquid with vigorous bubbling, and no residue was left in the container at the end of the test. The PMMA/SWNTs(0.5%) nanocomposite was solid-like and did not show noticeable bubbling except for a short period after initial exposure to the external radiant flux. The final residue, although having a slightly undulating surface, had no deep cracks and was slightly thinner than the original sample. The residue mainly consisted of SWNTs with a network structure that was porous, transmitting about 20% of the external radiant flux through the roughly 6-mm-thick layer[33]. On the other hand, numerous small island structures (black spots in Fig. 1c) were formed in the case of the PMMA/MWNTs(0.5%) and the islands coagulated with the progress of the test, leading to the formation of large islands having many deep cracks. Vigorous bubbling was observed through the cracks between the islands. Both the PMMA/CNFs(0.5%) and the PMMA/CBPs(0.5%) formed slightly viscous liquids, with vigorous bubbling occurring under heating. A thin, small, coagulated, network-like residue was left at the bottom of the container of the PMMA/CNFs(0.5%) and a thin black coating over the container surface with several small islands was left after the test on the PMMA/CBPs(0.5%), as shown in Fig. 1e.

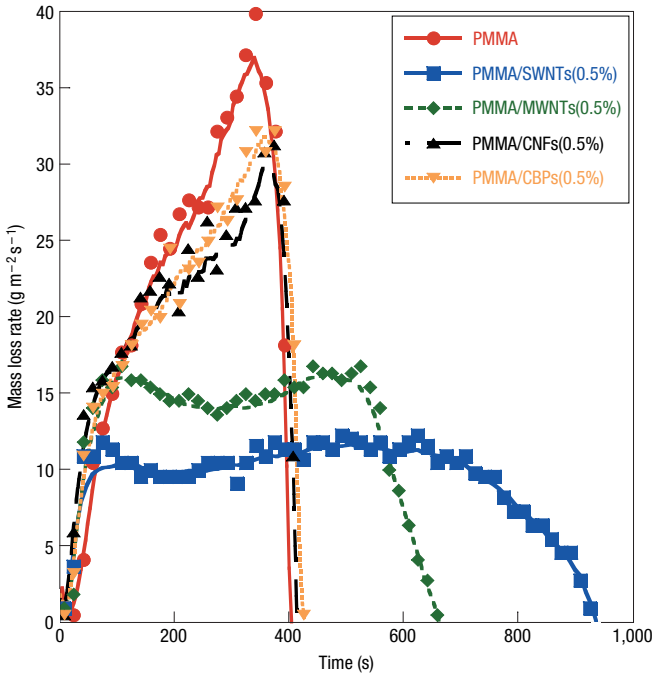

Figure 2 Effects of the nanoparticle type on mass loss rate. The tests were conducted at an external radiant flux of 50 kW m^{-2} in nitrogen.

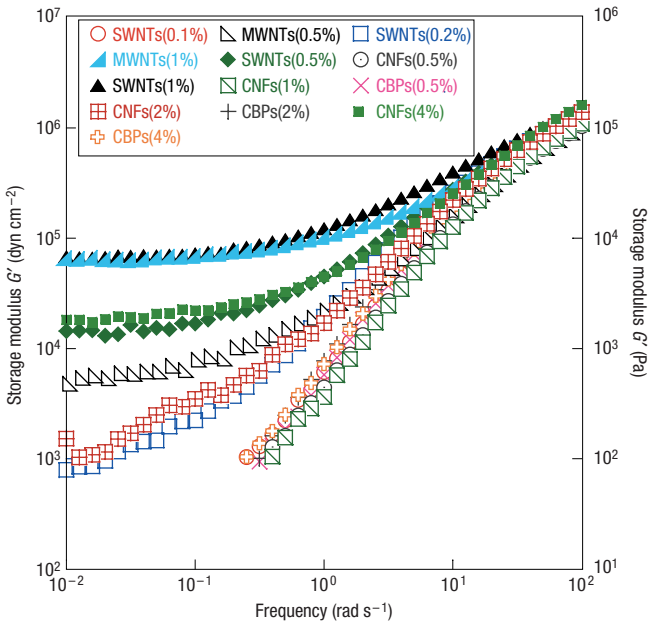

Figure 3 Effects of the nanoparticle type and concentration on the viscoelastic measurements. The samples with solid symbols show a gel behaviour at low frequencies.

The mass loss rate of each sample tested in the gasification test was calculated by taking the time derivative of the measured sample mass history; the results are plotted in Fig. 2. Only the PMMA/SWNTs(0.5%) formed the network-structured layer that suppressed bubbling; its mass loss rate was the least among the five samples, followed by the PMMA/MWNTs(0.5%). Mass loss rates of both the PMMA/CNFs(0.5%) and the PMMA/CBPs(0.5%) were not appreciably different from that of the pristine PMMA. From these observations, we clearly see that the formation of a network-structured protective layer during burning is crucial for the improvement in flammability properties, as suggested above.

To validate the hypothesis that a jammed network is formed in the initial samples, we performed viscoelastic measurements on the samples as a function of particle type and concentration. The viscoelastic properties of the PMMA nanocomposites containing SWNTs, MWNTs, CNFs or CBPs are presented in Fig. 3 for a range of filler mass fractions. The storage modulus G' provides a measure of nanocomposite 'stiffness' and its frequency dependence characterizes whether the material is in a liquid-like or solid-like state[24]. At 200 °C and low frequencies, the PMMA/CBPs composites have nearly the same rheological response as pure PMMA, regardless of the CBP concentration, showing the typical rheological response of a newtonian liquid behaviour with $G' \sim \omega^2$ (where ω is the oscillatory frequency) at low frequencies. This scaling was also observed for PMMA/CNFs nanocomposites with intermediate concentration loading (that is, 1%) and for nanocomposites with low loadings of these tubular fillers (that is, 0.1%). However, for the composites containing a higher concentration of these extended fillers, this liquid-like low-frequency scaling of G' disappeared and G' became nearly constant at low frequencies. This indicates a transition from a newtonian liquid to an ideal hookean solid, which accompanies the formation of a mechanically stable network structure[24,35] ('jammed network' or 'dispersion gel')[36]. We term the composition at which this rheological state is achieved the 'gel concentration', φ_g. Specifically, we define φ_g as the concentration at which G' becomes independent of ω for an extended low-frequency range.

In addition to the filler type and loading, the filler dimension also had a significant effect on the rheological response of the nanocomposite. With the same 0.5% filler loading, the SWNT nanocomposite had solid-like behaviour, whereas the MWNT nanocomposite had a much reduced elastic response as indicated by the smaller G' at low frequencies relative to the SWNT nanocomposite and the CNF nanocomposite showed only a liquid-like behaviour. An increase in the concentration of MWNTs and CNFs from 0.5% to 1% and 0.5% to 4%, respectively, yielded a gel-like rheological response for both MWNT and CNF nanocomposites. Our estimate of φ_g has the same order of magnitude as previously reported values of the percolation concentration for electrical conductivity (0.26 vol% (ref. 37) with SWNTs, and 1% (ref. 24) and 2% (ref. 38) with MWNTs), but our nanoparticle concentration is much less than the reported percolation threshold (a mass fraction of between 10% and 20%) for CNFs[39]. The addition of CBPs for the concentration range considered in this study did not lead to dispersion gelation. A relatively high percolation concentration of 9 vol% has been reported for CBPs[40].

Previous work has shown that there should be a general tendency of φ_g to decrease with decreasing tube diameter in this class of extended particles[36]. We can roughly understand this trend from the increase in the interfacial area and for tube of a smaller diameter. It is estimated that the interface areas of the MWNTs and the CNFs are about 70% and about 10% of that of the SWNTs, respectively, in 0.5% mass fraction of each type of tubes in PMMA. The fact that the SWNTs tend to form bundles or ropes of nanotubes mitigates the effect of having a small ratio of the SWNT diameter to the diameter of the MWNTs to some extent. The relationship between flammability properties and the total interfacial area is discussed in Supplementary Information.

The results of the gasification experiments with various concentrations of SWNTs, MWNTs and CBPs in PMMA are

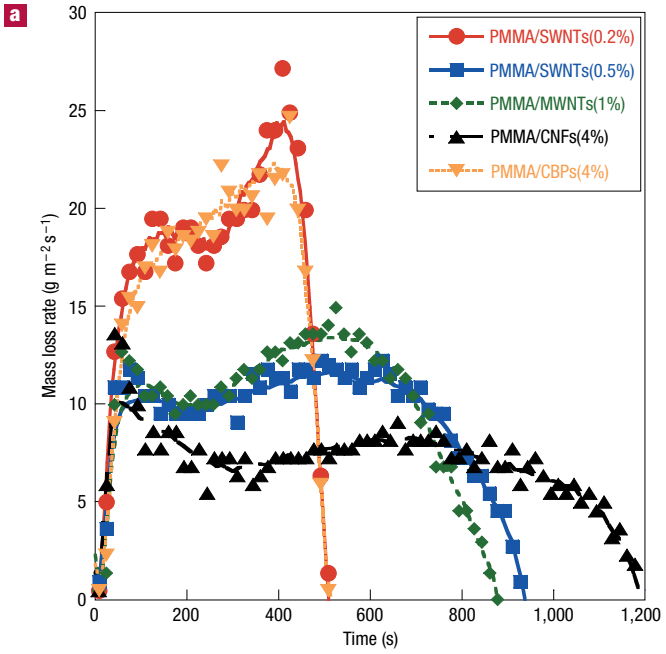

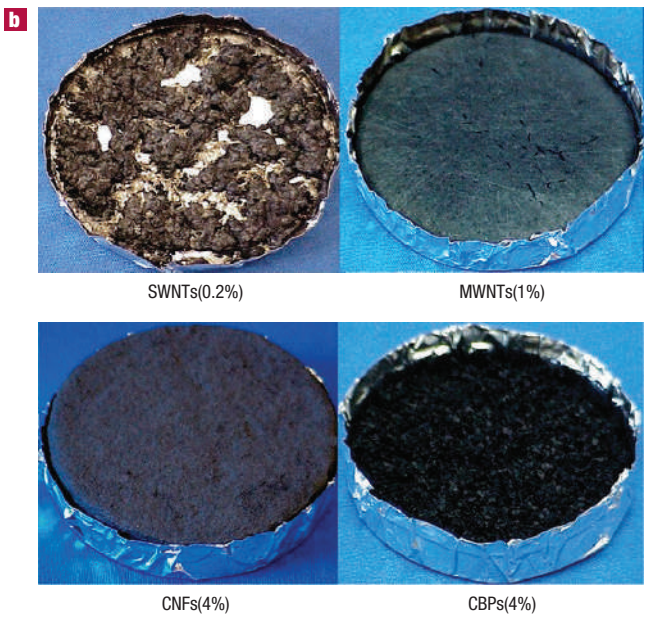

Figure 4 Effects of the nanoparticle type and concentration on mass loss rate and the configuration of the residues. The tests were conducted at an external radiant flux of 50 kW m^{-2} in nitrogen. **a**, Mass loss rate. **b**, Pictures of the residues.

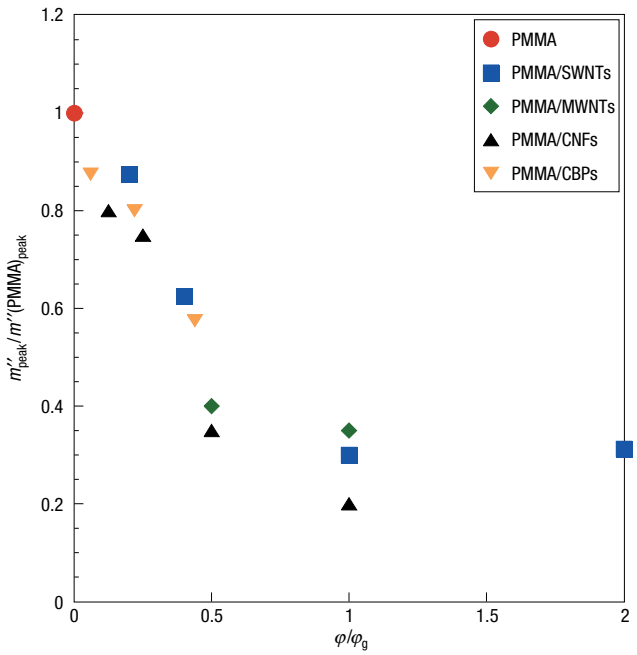

Figure 5 Relationships between normalized peak mass loss rate and normalized concentration of nanoparticles. Mass loss rates were measured at 50 kW m^{-2} in nitrogen. The peak mass loss rate is normalized by the peak mass loss rate of PMMA. The concentration is normalized by the concentration φ_g at which hookean solid gel is formed. The relationship of $m''_{peak}/m''(PMMA)_{peak} \approx 1-(2/3)(\varphi/\varphi_g)$ provides a fair representation of our data for the pre-gel concentration range, $0 \le \varphi/\varphi_g < 1$.

shown in Fig. 4a. The PMMA/SWNTs(0.2%), which did not form gelled nanocomposites (see Fig. 3), formed island structures (Fig. 4b) rather than a continuous network protective layer. Its mass loss rate was also much higher than that of the PMMA/SWNTs(0.5%), which formed a continuous protective layer. The PMMA/MWNTs(1%) and the PMMA/CNFs(4%) also formed a network layer (Fig. 4b) and their mass loss rates were at least as low as that of the PMMA/SWNTs(0.5%). However, the PMMA/CBPs(4%) formed a thin layer consisting of the accumulation of a large amount of coagulated granular particles. In addition, bubbling was observed between the granular particles; this sample's mass loss rate was as high as that of the PMMA/SWNTs(0.2%).

These observations indicate that a large reduction in nanocomposite flammability requires a sufficient nanoparticle concentration φ_g to form a jammed network within the polymer network. We next quantify how this flammability reduction depends on φ (the nanoparticle concentration) to show the transition between the low-flammability reduction regime for small φ and the high-flammability reduction regime for large φ. We normalize the nanoparticle concentration by φ_g for each type of nanoparticle. From Fig. 3 we estimate $\varphi_g = 0.5\%$ for SWNTs, 1% for MWNTs and 4% for CNFs. Although the CBP concentration used in this study was not sufficient for gelation, we chose a relatively large concentration of this filler ($\varphi_g = 9\%$) to compare with the extended nanoparticle additives. The relationship between the normalized concentration of nanoparticles and the normalized peak mass loss rate is shown in Fig. 5. The peak mass loss rate m''_{peak} is related to the peak heat release rate, which is a key flammability measure. This figure shows that an increase in the total surface area sharply decreases the peak mass loss rate until the nanocomposite reaches the critical composition φ_g. Then, it seems that a further increase in the concentration of the nanoparticle does not significantly affect the mass loss rate. (A further increase in the concentration of MWNTs in polypropylene actually increased the peak heat release rate, which is probably due to an increase in thermal conductivity of the nanocomposites[32].) These results confirm that achieving φ_g in the initial sample is critical for obtaining maximally reduced flammability properties. Apparently the network structure in the initial sample remains intact during burning, although it was compacted after the PMMA was degraded and its degradation products were gasified.

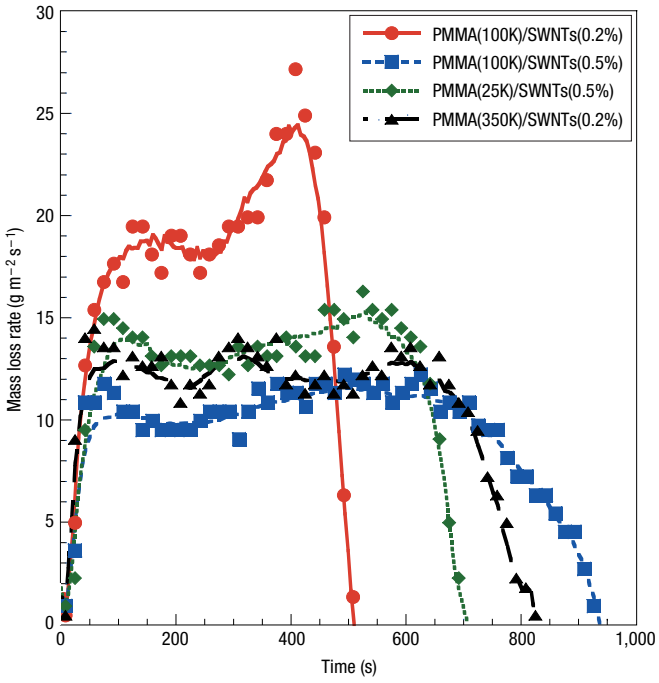

Figure 6 Effects of M_w of PMMA on mass loss rate. The tests were conducted at an external radiant flux of 50 kW m^{-2} in nitrogen.

The integrity of the network at high temperatures can be expected to be influenced by the molecular mass of the polymer matrix. We thus examine the effect of molecular mass, M_w, of the resin on the flammability properties of carbon-based nanocomposites. In particular, we anticipate that a high-M_w resin (high viscosity) enhances the formation of the network layer through entanglement couplings of the polymer chains with the nanotube bundles[33]. The low-M_w resin (low viscosity) should have a reduced network integrity owing to the destabilizing effect of the formation and convective motion of bubbles in the molten nanocomposite under burning conditions[34]. The movement of nanoclay particles induced by bubbles was observed in previous measurements on the gasification of polyamid 6–clay nanocomposites[15]. Similar effects could occur for the extended carbon-based nanocomposites if the integrity of the network is not sufficiently strong to resist the movement of bubbles. In order to examine the effects of M_w on the formation of a network and on flammability properties, PMMA nanocomposites (25,000 and 350,000 g mol^{-1}) were prepared with SWNTs; these were subjected to the rheological analysis. The G' of the PMMA(350K)/SWNTs(0.2%) was roughly an order of magnitude larger than that of the PMMA(100K)/SWNTs(0.2%) and it also showed a weak dependence on frequency in the range of low frequencies ($<10^{-1}$ rad s^{-1}). The G' of the PMMA(25K)/SWNTs(0.5%) was roughly an order of magnitude less than that of the PMMA(100K)/SWNTs(0.5%) and showed nearly the same dependence on ω as the PMMA(100K)/MWNTs(0.5%).

The measured mass loss rates of the PMMA(350K)/SWNTs(0.2%) and the PMMA(25K)/SWNTs(0.5%) are plotted in Fig. 6, including the PMMA(100K)/SWNTs(0.2%) from Fig. 4 and the PMMA(100K)/SWNTs(0.5%) from Fig. 2 for comparison. Mass loss rates of the nanocomposites with higher $M_w = 350{,}000$ g mol^{-1} PMMA were clearly lower than those with lower $M_w = 100{,}000$ g mol^{-1} PMMA. Even with 0.2% of SWNTs, the nanocomposites with $M_w = 350{,}000$ g mol^{-1} PMMA formed a very wavy, network-structured layer during burning compared with the formation of islands for $M_w = 100{,}000$ g mol^{-1} PMMA. At a mass fraction of 0.5% of SWNTs, the nanocomposite with $M_w = 25{,}000$ g mol^{-1} PMMA formed a network layer, but its mass loss rate was about 20% higher than that of the nanocomposite with $M_w = 100{,}000$ g mol^{-1} PMMA as shown in Fig. 6. Although the nanocomposites having the characteristic composition of φ_g are required for significantly reducing flammability properties, it seems that there is no direct correlation between G'_p (plateau in G' at low frequencies) at φ_g and the extent of flammability reduction with the nanoparticles. For example, the mass loss rate of the PMMA(100K)/SWNTs(1%) was about the same as that of the PMMA(100K)/SWNTs(0.5%) even though the former G'_p at φ_g was about four times higher than the latter G'_p. Furthermore, the PMMA(100K)/CNFs(4%) nanocomposite had the lowest mass loss rate, but its G'_p at φ_g was lower than those of PMMA/SWNTs(1%) and PMMA/MWNTs(1%) at φ_g.

The propensity to form jammed network structures from extended nanoparticles should not be limited to tubular-shaped additives and in future work we plan to examine our network hypothesis for the reduced flammability of polymer nanocomposites in the case of clay (plate) and carbon sheet additives. We also plan to investigate the role of particle flexibility and size polydispersity on the critical concentration φ_g describing the gel concentration. Finally, we point out that our observations suggest that we screen for promising flame-retarded polymer nanocomposites by performing viscoelastic measurements on the initially fabricated samples.

METHODS

Certain commercial equipment, instruments, materials, services or companies are identified in this article to specify adequately the experimental procedure. This in no way implies endorsement or recommendation by NIST.

The matrix polymer is PMMA (Polyscience). The SWNTs were synthesized by HiPCo and provided from Carbon Nanotechnologies Incorporated and Foster Miller Company. The MWNTs were purchased from Nano Laboratory and the CNFs (PR-I) were purchased from Applied Science. The CBPs were N299 provided by Sid Richardson Carbon. The coagulation method was used to produce all samples[35]. Dimethylformamide was chosen to dissolve the PMMA and to permit dispersion of the particles by sonication for 24 h. A concentration of 0.2 mg ml^{-1} (particles/dimethylformamide) was used to make sure that all of the samples had good dispersion of the particles in the sample. Rheology measurements were performed on a Rheometric Solid Analyzer (RSAII) in oscillatory shear with a sandwich fixture. Samples 12.5 mm × 16 mm × 0.5 mm were run at 200 °C with a strain of 0.5%. Results were reproducible after one frequency sweep, indicating that there was no chain degradation or further filler alignment during measurement.

A radiant gasification apparatus was designed and constructed at NIST to study the gasification processes of samples (75 mm diameter and 8 mm thick) by measuring sample mass and recording the sample behaviour using a video camera. The apparatus consists of a stainless-steel cylindrical chamber that is 1.70 m tall and 0.61 m in diameter. All tests were conducted at 50 kW m^{-2} in nitrogen; more detailed discussion of the apparatus is given in our previous study[41]. The standard uncertainty of the measured mass loss rate is ±10%. The peak mass loss rate m''_{peak} is related to the peak heat release rate, which is a key flammability measure. One peak was observed without the formation of a protective network layer, whereas two peaks were observed with samples having a jammed network, as shown in Figs 2 and 4a. The second, late-stage peak occurs after the formation of the protective network layer and in this case we chose this peak to define m''_{peak}.

Received 1 July 2005; accepted 18 August 2005; published 23 October 2005.

References

1. Kashiwagi, T. Polymer combustion and flammability — Role of the condensed phase. *Proc. Combust. Inst.* **28,** 1423–1437 (1994).
2. Clift, R., Grace, J. R. & Weber, M. E. *Bubbles, Drops, and Particles* (Academic, New York, 1978).

3. Kojima, Y. *et al.* Mechanical properties of nylon 6-clay hybrid. *J. Mater. Res.* **8,** 1185–1189 (1993).
4. Giannelis, E. P. Polymer layered silicate nanocomposites. *Adv. Mater.* **8,** 29–35 (1996).
5. Wang, Z. & Pinnavaia, T. J. Hybrid organic-inorganic nanocomposites: Exfoliation of magadiite nanolayers in an elastomeric epoxy polymer. *Chem. Mater.* **10,** 1820–1826 (1998).
6. Kashiwagi, T. *et al.* Thermal and flammability properties of a silica-poly(methylmethacrylate) nanocomposite. *J. Appl. Polym. Sci.* **89,** 2072–2078 (2003).
7. Gilman, J. W. & Kashiwagi, T. Nanocomposites: A revolutionary new flame retardant approach. *SAMPE J.* **33,** 40–46 (1997).
8. Gilman, J. W. *et al.* Flammability properties of polymer-layered-silicate nanocomposites. Polypropylene and polystyrene nanocomposites. *Chem. Mater.* **12,** 1866–1873 (2000).
9. Zhu, J., Morgan, A. B., Lamelas, F. J. & Wilkie, C. A. Fire properties of polystyrene-clay nanocomposites. *Chem. Mater.* **13,** 3774–3780 (2001).
10. Zanetti, M., Kashiwagi, T., Falqui, L. & Camino, G. Cone calorimeter combustion and gasification studies of polymer layered silicate nanocomposites. *Chem. Mater.* **14,** 881–887 (2002).
11. Gilman, J. W. Flammability and thermal stability studies of polymer layered-silicate (clay) nanocomposites. *Appl. Clay Sci.* **15,** 31–49 (1999).
12. Porter, D., Metcalfe, E. & Thomas, M. J. K. Nanocomposite fire retardants — A review. *Fire Mater.* **24,** 45–52 (2000).
13. Wilkie, C. A. in *Fire Retardancy of Polymers* (eds Le Bras, M., Wilkie, C. A. & Bourgiot, S.) Ch. 1 (Royal Society of Chemistry, Cambridge, 2005).
14. Kashiwagi, T. in *Fire Retardancy of Polymers* (eds Le Bras, M., Wilkie, C. A. & Bourgiot, S.) Ch. 6 (Royal Society of Chemistry, Cambridge, 2005).
15. Kashiwagi, T. *et al.* Flame retardant mechanism of polyamid 6-clay nanocomposites. *Polymer* **45,** 881–891 (2004).
16. Ajayan, P. M., Schadler, L. S., Giannaris, C. & Rubio, A. Single-walled carbon nanotube-polymer composites: strength and weakness. *Adv. Mater.* **12,** 750–753 (2000).
17. Park, C. *et al.* Dispersion of single wall carbon nanotubes by in situ polymerization under sonication. *Chem. Phys. Lett.* **364,** 303–308 (2002).
18. Chauvet, O., Benoit, J. M. & Corraze, B. Electrical, magneto-transport and localization of charge carriers in nanocomposites based on carbon nanotubes. *Carbon* **42,** 949–952 (2004).
19. Chang, T. E. *et al.* Microscopic mechanism of reinforcement in single-wall carbon nanotube/polypropylene nanocomposites. *Polymer* **46,** 439–444 (2005).
20. Stephan, C. *et al.* Raman spectroscopy and conductivity measurements on polymer-multi-walled carbon nanotubes composites. *J. Mater. Res.* **17,** 396–400 (2002).
21. Barrau, S., Demont, P., Peigney, A., Laurent, C. & Lacabanne, C. DC and AC conductivity of carbon nanotubes-polyepoxy composites. *Macromolecules* **36,** 5187–5194 (2003).
22. Ruan, S. L., Gao, P., Yang, X. G. & Yu, T. X. Toughning high performance ultrahigh molecular weight polyethylene using multiwalled carbon nanotubes. *Polymer* **44,** 5643–5654 (2003).
23. Meincke, O. *et al.* Mechanical properties and electrical conductivity of carbon-nanotube filled polyamide-6 and its blends with acrylonitrile/butadiene/styrene. *Polymer* **45,** 739–748 (2004).
24. Kharchenko, S. B., Douglas, J. F., Obrzut, J., Grulke, E. A. & Milger, K. B. Flow-induced properties of nanotube-filled polymer materials. *Nature Mater.* **3,** 564–568 (2004).
25. Lozano, K., Yang, S. & Zeng, Q. Rheological analysis of vapor-grown carbon nanofiber-reinforced polyethylene composites. *J. Appl. Polym. Sci.* **93,** 155–162 (2004).
26. Zeng, J., Saltysiak, B., Johnson, W. S., Schiraldi, D. A. & Kumar, S. Processing and properties of poly(methyl methacrylate)/carbon nano fiber composites. *Composites B* **35,** 173–178 (2003).
27. Xu, Y., Higgins, B. & Brittain, W. J. Bottom-up synthesis of PS-CNF nanocomposites. *Polymer* **46,** 799–810 (2005).
28. Gauthier, C., Chazeau, L., Prasse, T. & Cavaille, J. Y. Reinforcement effects of vapor grown carbon nanofibers as fillers in rubbery matrixes. *Compos. Sci. Technol.* **65,** 335–343 (2005).
29. Peeterbroeck, S. *et al.* Polymer-layered silicate-carbon nanotube nanocomposites: unique nanofiller synergistic effect. *Compos. Sci. Technol.* **64,** 2317–2323 (2004).
30. Beyer, G. Filler blend of carbon nanotubes and organoclays with improved char as a new flame retardant system for polymers and cable applications. *Fire Mater.* **29,** 61–69 (2005).
31. Kashiwagi, T. *et al.* Thermal degradation and flammability properties of poly(propylene)/carbon nanotube composites. *Macromol. Rapid Commun.* **23,** 761–765 (2002).
32. Kashiwagi, T. *et al.* Thermal and flammability properties of polypropylene/carbon nanotube nanocomposites. *Polymer* **45,** 4227–4239 (2004).
33. Kashiwagi, T. *et al.* Flammability properties of polymer nanocomposites with single-walled carbon nanotubes: effects of nanotube dispersion and concentration. *Polymer* **46,** 471–481 (2005).
34. Schartel, B., Pötschke, P., Knoll, U. & Abdel-Goad, M. Fire behavior of polyamide 6/multiwall carbon nanotube nanocomposites. *Eur. Polym. J.* **41,** 1061–1070 (2005).
35. Du, F. *et al.* Nanotube networks in polymer nanocomposites: rheology and electrical conductivity. *Macromolecules* **37,** 9048–9055 (2004).
36. Bicerano, J., Douglas, J. F. & Brune, D. A. Model for the viscosity of particle dispersions. *J.M.S.-Rev. Macromol. Chem. Phys. C* **39,** 561–642 (1999).
37. Hough, L. A., Islam, M. F., Janmey, P. A. & Yodh, A. G. Viscosity of single wall carbon nanotube suspensions. *Phys. Rev. Lett.* **93,** 168102 (2004).
38. Pötschke, P., Fornes, T. D. & Paul, D. R. Rheological behavior of multiwalled carbon nanotube/polycarbonate composites. *Polymer* **43,** 3247–3255 (2002).
39. Lazano, K., Yang, S. & Zeng, Q. Rheological analysis of vapor-grown carbon nanofiber-reinforced polyethylene composites. *J. Appl. Polym. Sci.* **93,** 155–162 (2004).
40. Yurekel, K. *et al.* Structure and dynamics of carbon black-filled elastomers. *J. Polym. Sci. B* **39,** 256–275 (2001).
41. Austin, P. J., Buch, R. R. & Kashiwagi, T. Gasification of silicone fluids under external thermal radiation Part 1. Gasification rate and global heat of gasification. *Fire Mater.* **22,** 221–237 (1998).

Acknowledgements

We thank S. Kharchenko of Masco Corporation for valuable discussion and Carbon Nanotechnologies Incorporated, Foster Miller Company for providing SWNTs and Sid Richardson Carbon Company for providing CBPs. T.K. acknowledges funding from NIST by 5D1022 and F.D. and K.I.W. acknowledge funding from the Office of Naval Research by ONR Grant N00014-03-1-0890. This is a publication of the National Institute of Standards and Technology (NIST), an agency of the US Government, and by statute is not subject to copyright in the United States.
Correspondence and requests for materials should be addressed to T.K. or J.F.D.
Supplementary Information accompanies this paper on www.nature.com/naturematerials.

Competing financial interests

The authors declare that they have no competing financial interests.